JTTEE5 17:974–982
DOI: 10.1007/s11666-008-9269-y
1059-9630/$19.00 © ASM International

Asymmetric Melting Behavior in Twin Wire Arc Spraying with Cored Wires

W. Tillmann, E. Vogli, and M. Abdulgader

(Submitted June 9, 2008; in revised form September 26, 2008)

Asymmetric melting behavior of the electrodes is a process-related feature of the Twin Wire Arc Spraying (TWAS) technique since the heating of the negative connected wire is different from that of the positive connected wire. Due to these differences in melting behavior, a tracking of particle velocity and temperature for both electrodes individually is very important. Particle velocity and temperature have been recorded from anode side and cathode side by positioning the tracking device respectively. To draw the whole picture of the spraying, jet, particles have been tracked also from the top side of the spray gun. The goal of this study is to have an experimental data setup for model building and simulation of depositing process in TWAS. Corresponding measuring devices have been employed to investigate the TWAS process by spraying of massive and cored wires.

Keywords diagnostics and control, influence of process parameters, spray deposition

1. Introduction

Thermal spraying is a generic term for a group of coating processes that deposit finely divided (like in plasma or HVOF) or atomized (like in twin wire arc spraying) metallic or nonmetallic spraying material. These processes differ in their thermal source and in their feedstock. The three major categories of feedstock define the form of the spraying material used: powder, massive wires, and cored wires. The size of in-flight particles is predefined by powder size distribution in case of powder feedstock. The powder particles are finely divided by means of carrier gas and subsequently through the heat source in plasma or HVOF. In twin wire arc spraying (TWAS), a spray is formed by atomization of molten or semimolten droplets by the impingement of fast moving and continuously flowing atomization gas upon melting tips of consumable and electrical conductive wires. The wires are connected individually as anode and the other one as cathode and fed together to ignite an arc at the shortest distance between the electrical conductive part in wire tips.

The asymmetric melting behavior of massive wires was observed using similar or different wires in many studies (Ref 1-5). It is well known that the anode and cathode are heated differently in a TWAS process (Ref 2, 4, 5). The arc attaches to the anode over a larger area than the cathode. The heating is more localized at cathode and appears as cathode spot (Ref 3, 4, 6, 7). At the tip of the anode wire a large area is heated due to diffuse arc-anode attachment, melting a layer of metal that is pushed off the edge of the wire tip by the atomizing gas, creating an ''anode sheet.'' At the cathode, constricted arc attachment causes much more localized heating and melting (Ref 1-3). The asymmetric melting behavior of anode and cathode together with the arc fluctuation, due to periodic removal of molten material, affects consequently the in-flight particle characteristics. In-flight particle characteristics such as velocity, temperature, and size are controlling factors in splat formation, layer evolution, and in determination of the coating quality in thermal spraying technique (Ref 6-12).

Since in TWAS the particles are atomized from the bath of melting material in the arc zone, their size is not predictable and is dependent on the process parameters and the material properties of the wires. The use of cored wires has enhanced the coating quality of TWAS regarding wear resistance. The composition of the cored wires is inhomogeneous. It contains electrical conductive solid velum and a powder filling, which strongly influences the particle formation and in-flight particle characteristic data (Ref 13, 14).

The aim of this study is to develop a more fundamental understanding of the interactions between asymmetric melting behavior in TWAS process, independent process parameter, and in-flight particle catachrestic data by using cored wires. A comparison with massive wire is made to

This article is an invited paper selected from presentations at the 2008 International Thermal Spray Conference and has been expanded from the original presentation. It is simultaneously published in *Thermal Spray Crossing Borders, Proceedings of the 2008 International Thermal Spray Conference*, Maastricht, The Netherlands, June 2-4, 2008, Basil R. Marple, Margaret M. Hyland, Yuk-Chiu Lau, Chang-Jiu Li, Rogerio S. Lima, and Ghislain Montavon, Ed., ASM International, Materials Park, OH, 2008.

W. Tillmann, E. Vogli, and **M. Abdulgader**, Institute of Materials Engineering, Dortmund University of Technology, Dortmund, Germany. Contact e-mail: wolfgang.tillmann@udo.edu.

see the effect of the filling powder in cored wires on these phenomena.

The correlations between the abovementioned subjects of study will help to better predict the coating quality, make the spraying process more reliable, improve the reproducibility of desired coating, and give the conditions of spraying process simulation.

2. Materials and Experiments

2.1 Materials

Smart Arc 350 PG (Sulzer Metco, Switzerland) was used to investigate the particle formation and in-flight particle characteristics. The investigations were carried out on two types of wires with a diameter of 1.6 mm: cored wires (AS850, Co. Durum, Cr 4%, Mn <1%, Si 1,4%, C 2%, WSC 50%, Fe Bal, particle grain sizes 35-75 μm of the filling powder) and massive wires (Co.GTV, Ni. 99.9%).

2.2 Experiments

Design of Experiment (DoE) is useful in reducing the number of experiments required to optimize thermal spraying process (Ref 1, 12, 13). The primary purpose of the DOE screening objective is to select or to screen out the few important main effects from the many less important ones. These screening designs are also termed main effect designs. The approach chosen in this study is described as two-level full factorial designs with center point (Fig. 1).

In this study the Independent Controllable Process Parameters (ICPP) were assigned to atomization, arc voltage, and arc current (higher current higher wire feed rate). Atomization is the arrangement between Primary and Secondary atomization Gas pressure (PG_SG). Three evenly spaced low, center and high preset values denoted −1, 0, and 1, respectively, were chosen for each ICPP. The values for ICPP are as following:

- Atomization gas pressure in Bar (PG_SG) (−1, 0, +1) (2_0, 4_3, 6_6), respectively
- Arc voltage in Volt (−1, 0, +1) (28, 31, 34), respectively
- Arc current in Ampere (−1, 0, +1) (180, 220, 260), respectively

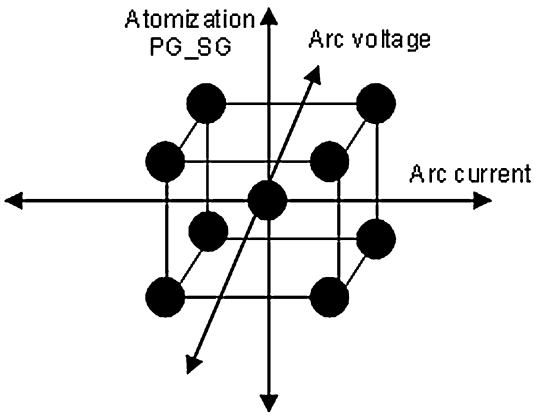

Fig. 1 Schematic diagram showing two-level full factorial design with center point used for this study

Experiments were performed using the combinations of ICPP settings corresponding to the eight points at the cube cell corners (−1, 1, −1), (1, 1, −1), (−1, −1, −1), (1, −1, −1), (−1, 1, 1), (1, 1, 1), (−1, −1, 1), (1, −1, 1) and the cube center point (0, 0, 0). The center point setting was executed at the middle and at the end of the experimental setup. Three complete experimental setups were implemented at standoff distances of 45, 100, and 150 mm along the axial spray cone on Anode (A) side as well as on Cathode (C) side. The center point setting was performed at axial standoff distances beginning from 30 to 150 mm in a 10 mm step. To verify the asymmetry in spray jet, a radial scanning of in-flight particles along the axial standoff distances was carried out. In doing so, an additional measurement with the center point setting was taken at the intersection between anode and cathode at axial standoff distances in the rage of 30 to 150 mm with a 10 mm step.

The numbering of experiments consists of a capital letter. It gives the measuring device position: ''A'' for anode side, ''C'' for cathode side, and ''O'' for the intersection between anode and cathode. The letter followed by a number combination reveals the ICPP setting for arc voltage-Atomization gas pressure-arc current.

For example A_28_2-0_180 means anode side, voltage 28 V, primary gas 2 bar, secondary gas 0 bar, and current 180 A.

2.3 Diagnostic

To determine the in-flight particle velocity and temperature AccuraSpray-g3 (Tecnar, Canada) was used, which consists of sensor head and controller unit (Fig. 2).

The principle behind AccuraSpray is based on optical means. Particle velocities are obtained from cross-correlation of signals which are recorded at two locations. In addition, the detectors are filtered at two different colors allowing the mean particle temperature to be measured using the very well-known twin wavelength pyrometry principle (assumes that the emissivity of the particles is the same for the two wavelengths). The AccuraSpray-g3 provides ensemble average data representing the particle temperature and velocity in a measurement volume of approx. Ø3 mm * 25 mm (Ref 15). The accuracy of the AccuraSpray measurements reaches 2% for particle temperature and 0.5% for particle velocity according to the product data sheet of the manufacturer.

As shown in Fig. 3 the AccuraSpray sensor head was located alternatively along the positively charged wire (anode) side, negatively charged wire (cathode) side, and along the intersection between electrodes. Different

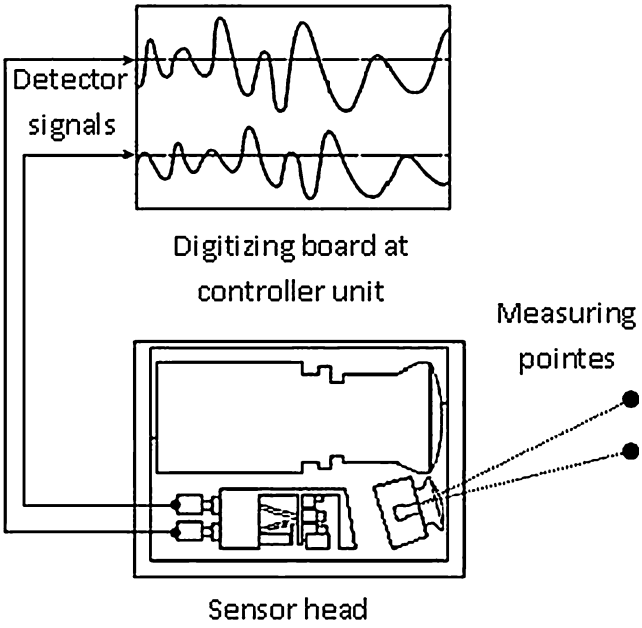

Fig. 2 Principles behind AccuraSpray

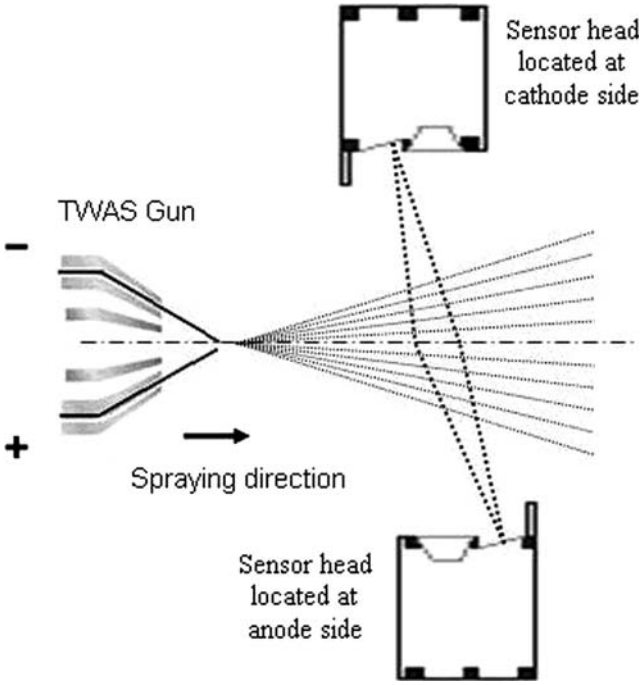

Fig. 3 Positioning of sensor head along the spraying axes on cathode side, anode side, and on intersection of electrodes at different standoff distances

parameter setups were tested at several standoff distances along the main spraying axis. Particle velocity and temperature have been recorded for every single experimental setup. The collected data have been analysed and conclusions of the different evaluated experimental setups have been drawn.

3. Results

Because of asymmetry of the electrical arc itself and the resulting differences in melting behavior of anode and cathode, the spray jet exhibited asymmetric radial variation of both particle velocity and temperature, which make a radial investigation by additionally measuring along the intersection between anode and cathode unavoidable.

3.1 Variations in Particle Temperature and Velocity for all ICPP Settings

Figure 4 shows a decrease in the temperature of cathode side particles with increasing standoff distances, and a simultaneous increase in the temperature of anode side particles. Due to the heat exchange between the particles in-flight, a declination of the temperature discrepancy between anode side particles and cathode side particles was revealed at higher standoff distances. The deposited particles are conveyed in an air jet, which has a conical shape. The air jet moves with high velocity through the surrounding environment and can be regarded as adiabatic conveying cells. Each cell consists of particles with different temperature surrounded by conveying air jet. Inside the adiabatic conveying cells a heat exchange occurred between the particles. The particles from anode side and cathode side reached approximately the same temperature at 150 mm standoff distance. In general the variation in particle temperature from anode side and cathode side was higher in the case of massive wire. The particles from massive wire had a slightly higher temperature at lower standoff distances between 45 and 100 mm. In higher standoff distances, a higher decrease in particle temperature was recorded using massive wire. Particle temperature of cored wire was slightly higher at 150 mm standoff distance. A variation in temperature was observed between anode side particles and cathode side particles. At standoff distances smaller than 100 mm, a higher particle temperature variation (200 to 400 °C) was recorded at the different ICPP settings and for both wire types.

The particle velocity increased at all ICPP settings with increasing axial standoff distance. A maximum velocity was reached at a standoff distance between 100 and 150 mm. The particles generated from massive wires (MW) attained about 20 to 30% higher velocity then the ones from cored wires (CW). At a lower ICPP setting, a variation in particle velocity between anode side and cathode side was recorded for both wire types. At a higher ICPP setting, a deviation in particle velocity appeared clearly. It was stated that the particles from cathode side has a 10% higher velocity compared to the ones from anode side for both wire types. There was a clear velocity gap for the particle velocity of cored wire at different ICPP settings. Particles from massive wire showed a different behavior. A higher velocity gap was recorded by changing the ICPP setting from low to middle, while a slight variation in particle velocity was obtained in lower standoff distance by changing the ICPP from middle to high.

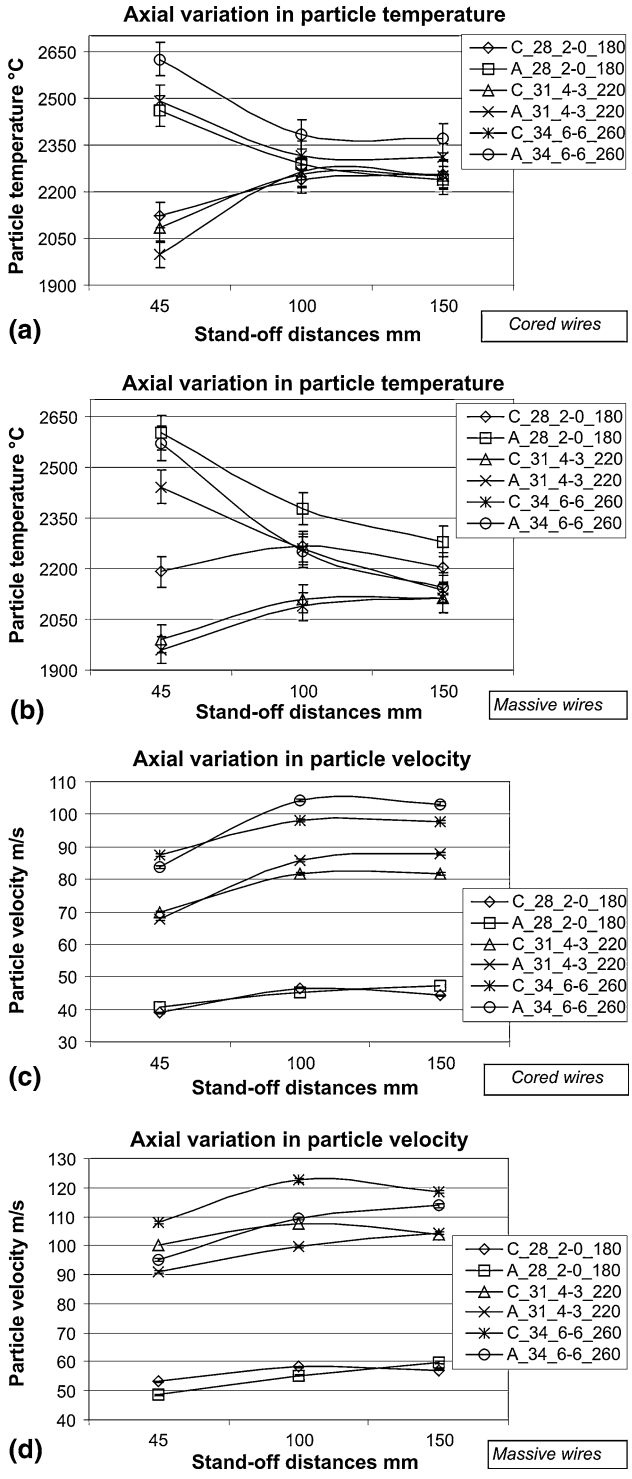

Fig. 4 Behaviour of in-flight particles by the different settings (a) and (b) particle temperature (c) and (d) particle velocity (A anode side/C cathode side/_voltage_primary gas-secondary gas_current)

3.2 Axial Variations Due to Arc Voltage

As expected, an increase of particle temperature (Fig. 5) was recorded as arc voltage was increased for both

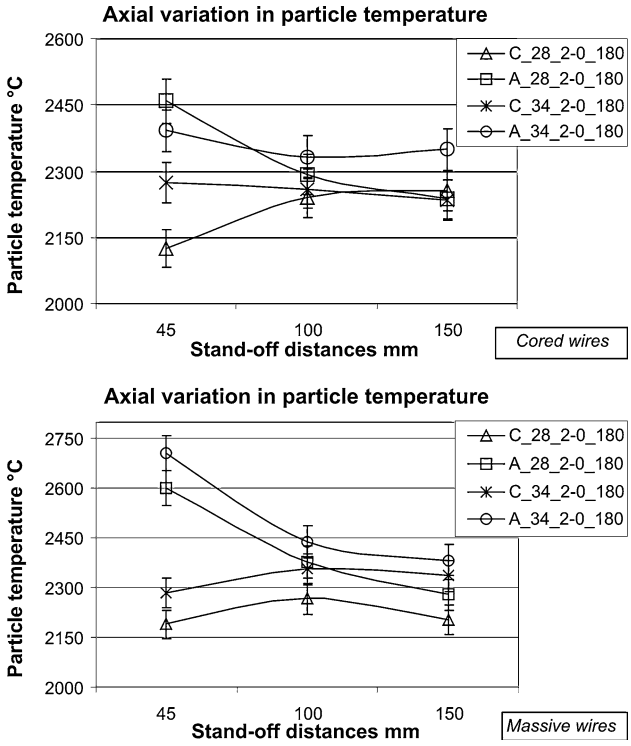

Fig. 5 Variation in particle temperature due to the change in arc voltage (A anode side/C cathode side/_voltage_primary gas-secondary gas_current)

cathode side and anode side, as well as for both wire types. The temperature divergence between anode side particles and cathode side particles was higher by spraying massive wires compared to cored wires.

At higher arc voltage and at smaller standoff distances, a lower heat exchange takes place compared to the lower voltage setting. This can be explained to be due to higher starting temperatures at higher voltage settings. The particle temperature increased about 50 to 100 °C at a standoff distance of 150 mm by increasing the voltage from 28 to 34 V. Lower arc voltage results in a higher particle temperature difference between anode side and cathode side for both wires.

Figure 6 shows a reduction of particle velocity at a higher arc voltage setting by using massive wires for particles generated in the anode side and cathode side. The velocity decreases approximately 10 m/s along the axial standoff distances. The velocity reduction can be explained to be due to larger particle size generated by higher voltage setting. In the case of massive wires, the melted (heated) area is larger than in cored wires. In cored wires, the powder inside the velum affects strongly the size of initiated particles.

3.3 Axial Variations due to Arc Current

It is seen from Fig. 7(a) and (b) that by increasing of arc current has a negligible effect on the temperature of anode side particles and cathode side particles for both wire types. The temperature of cathode side particles

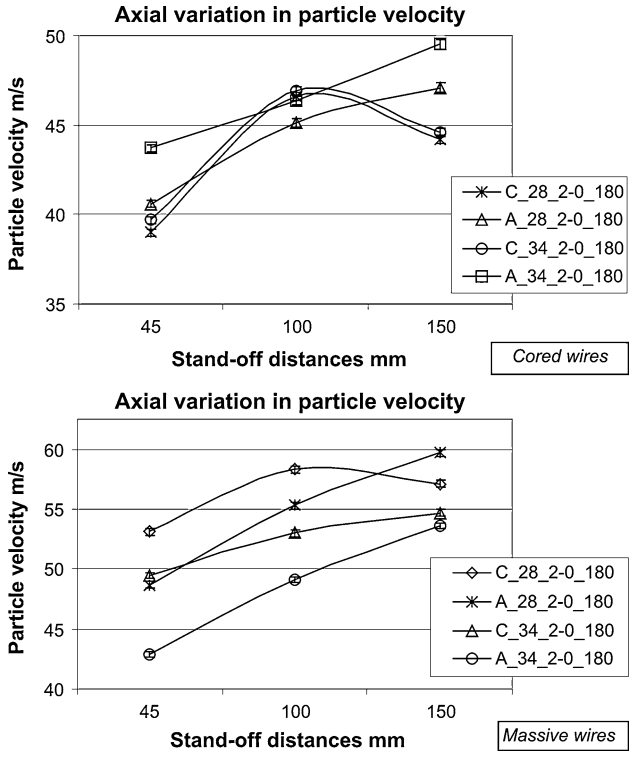

Fig. 6 Variation in particle velocity due to the change in arc voltage (A anode side/C cathode side/_voltage_primary gas-secondary gas_current)

obtained is found to be similar at higher arc current 260 A for both wires at lower standoff distances (45 to 60 mm). The same results were reported by Hale et al. in (Ref 7). The magnitude of current changes is not big enough to record high changes in particle temperature.

The particle velocity of both wires and both electrodes was decreased (Fig. 7c and d) with the increase of arc current from 180 to 260 A. No significant changes were recorded for both wire types and both electrodes with the increase of arc current. A slight decrease in particle velocity was obtained for both wires at 150 mm standoff distance.

It is observable that the particles from cathode side and anode side sprayed by massive wires showed higher temperatures and higher velocities then those sprayed by cored wires.

3.4 Effects of the Atomization Gas Pressure

The atomization was realized by combining primary and secondary atomization gases together (PG_SG). Figure 8 shows that increasing of atomization gas pressure considerably increases particle velocity at anode side and at cathode side. The particle velocity at anode side for both wire types increased linearly along the axial distances between 45 and 150 mm and reached its maximum at 150 mm. A linear increase at standoff distances between 45 and 100 mm was recorded for the cathode side too. The particles reached their highest velocity at 100 mm,

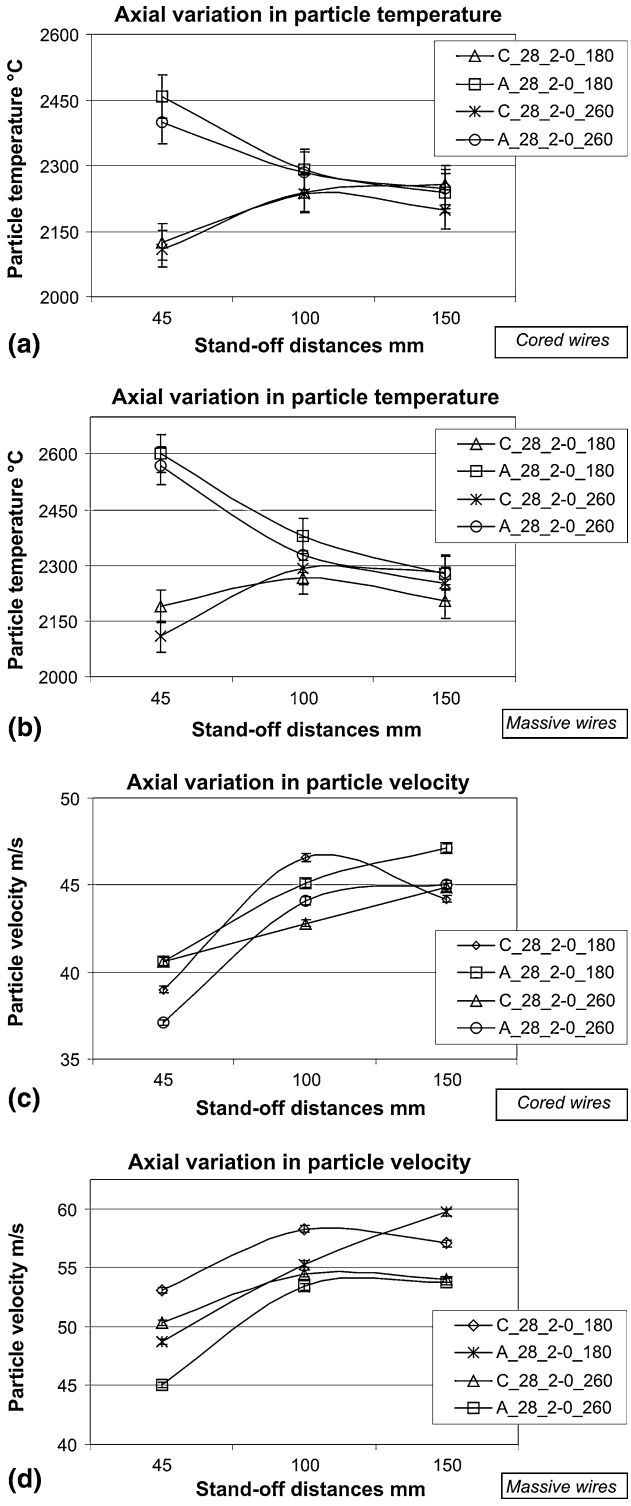

Fig. 7 Behavior of in-flight particles due to the change in arc current (A anode side/C cathode side/_voltage_primary gas-secondary gas_current)

followed by a slight decrease at 150 mm standoff distance in the case of cored wires and remained constant in massive wires. There was a negligible velocity gap between

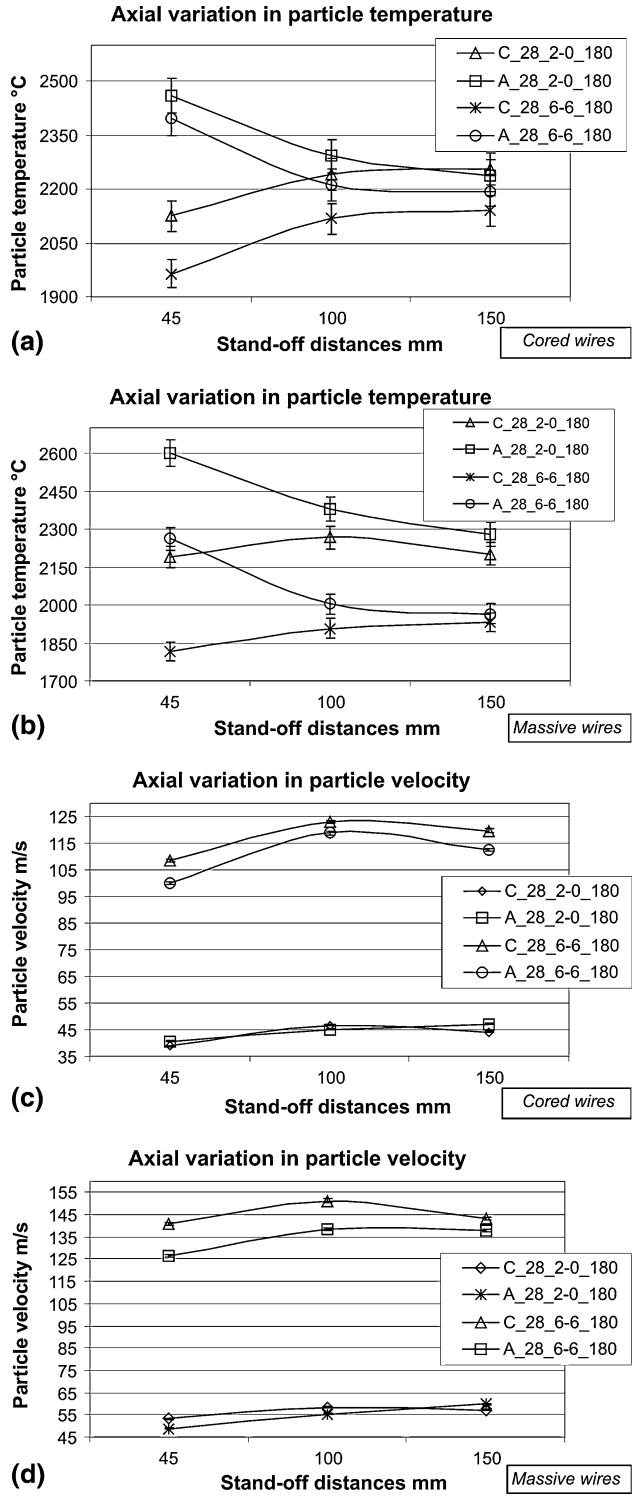

Fig. 8 Behavior of in-flight particles due to the change in atomization pressure PG_SG (A anode side/C cathode side/ _voltage_primary gas-secondary gas_current)

anode particles and cathode particles for both wire types at lower atomization gas pressure.

At a higher atomization setup, a higher velocity gap was obtained between anode side particles and cathode side particles for both wires. The particles from cored wires reached their highest velocity at 100 mm standoff distance; afterward a decrease of about 10% occurred. Approximately 20 to 25 m/s higher particle velocity was obtained by using massive wires for particles at anode side as well as at cathode side.

A lower particle temperature was reported for the higher atomization setup. The reason was the higher cooling rate due to the higher gas flow rate. In general, the cooling rate of the particles sprayed with lower atomization setup along the standoff distances was higher compared to particles sprayed by higher setting. The reason was the lower particle velocity of the lower atomization setup resulted in longer flying time.

Particles from cored wire revealed a higher temperature than the particles from massive wire at the higher atomization setting for both electrodes. In lower it setting was the other way around.

The velocity discrepancy at higher setting was larger for massive wire than for cored wires. The velocity variation at 100 mm standoff distance between particles generated from anode and the ones from cathode was 5 and 14 m/s for cored wire and massive wire, respectively.

3.5 Behavior of In-Flight Particles in Axial and Radial Direction

The setting of the cube center point was used for these experiments with the following combination: arc voltage 31 V, atomization primary gas 4 bar, secondary gas 3 bar and, arc current 220 A (31_4-3_220). Recording of particle velocity and temperature was made at different standoff distances from 30 to 150 mm in 10 mm step. The recording device was located one along the anode, one along the cathode, and one along the intersection point between anode and cathode. The axial setup confirmed the previous results. In addition to the axial variation, there was a radial variation at every standoff distance. The radial variation decreased with increasing axial standoff distances.

Figure 9 shows a temperature gap between anode side particles and cathode side particles. In the case of cored wires a smaller gap was recorded. It decreased at standoff distance of 60 mm and reached its minimum at about 90 mm. The particles from massive wires revealed a larger discrepancy between anode side and cathode side particles. The discrepancy got smaller at higher standoff distances when compared to cored wires (at about 90 mm) and reached its minimum at 130 mm standoff distance.

The particle velocity of cored wires and massive wires showed the same behavior as in the case of temperature. The velocity gap between anode side particles and cathode side particles was smaller by using cored wires. In general, it can be stated that the particles generated from cored wires revealed a lower radial variation in temperature and velocity along the entire axial standoff distances than those generated from the massive wires. The spray jet of cored wires was supposed to be more homogeneous with respect to the smaller discrepancy in particle temperature and velocity.

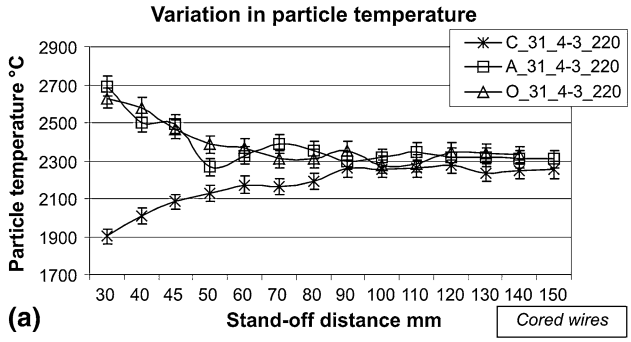

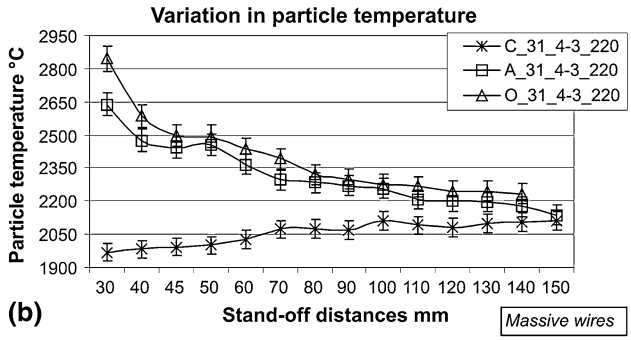

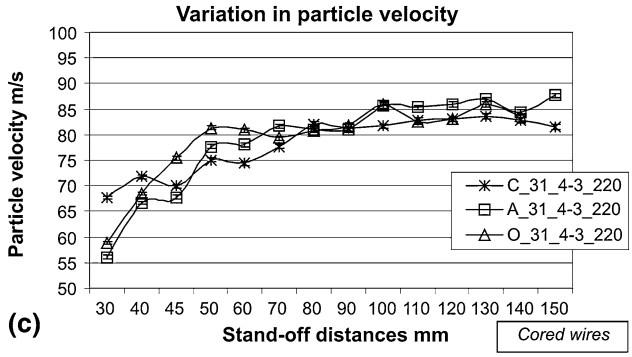

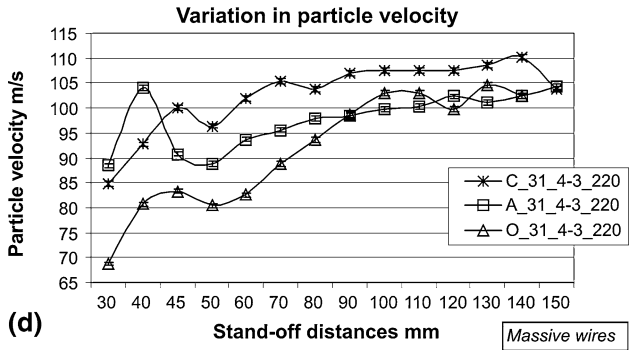

Fig. 9 Axial and radial behavior of in-flight particles (A anode side/C cathode side/O intersection voltage_primary gas-secondary gas_current)

4. Discussion

With the use of design of experiment (DoE), the interactive effects of ICPP on the axial and radial variation of particle velocity and temperature for anode and cathode can be thoroughly explored (Table 1). The variation in particle temperature and particle velocity between cathode side and anode side for both wires was computed as follows:

$$\begin{aligned} \text{CAi} &= (1/4)\,(\text{S responses at high setting}) \\ &\quad - (1/4)\,(\text{S responses at low setting}) \end{aligned}$$

$$\begin{aligned} \text{CCi} &= (1/4)\,(\text{S responses at high setting}) \\ &\quad - (1/4)\,(\text{S responses at low setting}) \end{aligned}$$

where (i) indicates one of the ICPP parameters:

CA1: Responses at anode side for voltage setting

CA2: Responses at anode side for atomization gas pressure setting

CA3: Responses at anode side for atomization gas pressure setting

CC1: Responses at cathode side for voltage setting

CC2: Responses at cathode side for atomization gas pressure setting

CC3: Responses at cathode side for atomization gas pressure setting

Variance factor for each ICPP = |CAi − CCi|.

The calculations were done for all standoff distances for both wires and at the cathode side as well as at anode side. The values in Table 1 are the results obtained at 45 and 100 mm standoff distances and show the effect of ICPP setting on the velocity gap and temperature gap between particles from cathode and particles from anode. The values in Table 1 show the inhomogeneity factor (the higher the inhomogeneity factor, the bigger the gap between anode and cathode) for particle temperature and particle velocity in the spraying jet at different ICPP settings. The results in Table 1 confirmed that the TWAS spraying jet is an inhomogeneous spray jet with respect to particle velocity and temperature.

The results clearly showed that the atomization pressure was the predominant ICPP affecting particle velocity; it was found that high atomization pressure exerted a cooling effect at lower axial standoff distances. An increase of particle velocity along the axial standoff distance was revealed by all ICPP settings. The increase of particle velocity is related to the secondary atomization at standoff distances close to the arc zone up to 50 mm away from the arc, which is in agreement with the results from earlier studies (Ref 3, 4, 6, 8).

Particles from cored wires revealed a higher temperature than the particles from massive wires with higher atomization setting for both electrodes. In lower setting it was the other way around.

On wire tips in twin wire arc spraying, there are two kinds of energy impact. Firstly, a continuously dynamic force was applied by atomization gas. Its magnitude is directly affected by gas pressure. Secondly, a heating energy caused by a fluctuating electrical arc stroked between the anode and cathode and its magnitude is affected by arc

Table 1 Effect of ICPP setting on particle temperature gap and on particle velocity gap between (A) anode and (C) cathode for CW cored wire and MW massive wire (inhomogeneity value in spraying jet)

	T-gap A-C				V-gap A-C			
	CW		MW		CW		MW	
Variance value	**@45**	**@100**	**@45**	**@100**	**@45**	**@100**	**@45**	**@100**
ICPP setting								
Arc voltage	113.5	91.8	492.2	127.3	3.8	2.7	9.5	8.4
Atomization gas pressure	563.5	112.3	509.5	130.9	6.5	3.4	13.7	11.7
Arc current	442.1	78.8	499.6	113.5	3.9	2.1	10.1	7.1

voltage and arc current. The arc fluctuation is caused by the material removal from wire tips by means of atomization gas and the continuous feed of wire into the arc zone. This leads to ignition followed by extinction and reignition in periodic time of milliseconds. The atomization gas force deforms the wire tips material as soon as its tensile strength decreased by arc heating. The dynamic forces due to continuously flowing atomization gas causes elongation of wire tips material. The material must not be fully molten. The material sheared and formed the so-called anode sheet and cathode sheet (Ref 1, 2). The anode sheet is different from the cathode sheet due to the different attachment of arc to the anode and cathode. The length and form of the abovementioned sheets are strongly affected by the atomization gas pressure, arc voltage, and arc current. The heat impact on the formed sheets continued due to arc reignition.

In the case of cored wires, the material removal occurs at electrical conductive velum on the inside of wires at first. Therefore, the electrical nonconductive filling powder, which is not a part of arc ignition, is exposed to excessive heating by arc ignition and to erosion by continuously flowing atomization gas. Because of arc fluctuation and continuous erosion, a considerable part of filling powder does not melt and will be wetted or impregnated into molten velum material during their flight to the substrate. It is supposed that this phenomena is different in the cathode and the anode.

5. Conclusions

The evaluation of particle velocity and temperature by twin wire arc spraying was carried out on cored and massive wires. The recordings were taken by measuring at different standoff distances at the anode side and at the cathode side. The radial variations of both particle velocity and temperature were revealed by adding an axial measurement setup along the intersection point between the anode and cathode. It was found that the velocity did not increase in the same magnitude as the primary gas and/or secondary gas. The highest particle acceleration took place from arc ignition up to 50 mm standoff distance. At standoff distances between 100 mm and 150 mm, the velocity reached its maximum value. Furthermore the velocity of particles generated by spraying of cored wires is about 30% smaller than that of particles generated by spraying of massive wire.

Cooling effects of PG and SG have been recorded on measurements carried out at both wires. The temperature of particles generated from massive wire is higher than that of particles generated from of cored wire at almost all ICCP settings. An exception is the particles generated at high atomization gas setup, in which the particle temperature of cored wires is higher than that of the massive wires.

Based on the results of the diagnostics of TWAS process an accurate simulation of spraying process can be established. This will lead to an improvement of the coating properties and surface quality, which can be used to improve the coating quality for tool surfacing.

Acknowledgments

The authors gratefully acknowledge the financial support of the DFG (German Science Foundation) within the Collaborative Research Center SFB 708.

References

1. N.A. Hussary and J.V.R. Heberlein, Effect of System Parameters on Metal Break-Up and Particle Formation in the Wire Arc Spray Process, *J. Thermal Spray Technol.*, 2007, **16**(1), p 1-13
2. N.A. Hussary and J.V.R. Heberlein, Atomization and Particle-Jet Interactions in the Wire-Arc Spraying Process, *J. Thermal Spray Technol.*, 2001, **10**(4), p 604-610
3. T. Watanabe, T. Sato, and A. Nazi, Electrode Phenomena Investigation of Wire Arc Spraying for Preparation of Ti-Al Intermetallic Compounds, *Thin Solid Films*, 2002, **40**(7), p 98-103
4. T. Watanabe, X. Wang, E. Pfender, and J. Heberlein, Correlations Between Electrode Phenomena and Coating Properties in Wire Arc Spraying, *Thin Solid Films*, 1998, **316**, p 169-173
5. Y.L. Zhu, H.L. Liao, C. Coddet, and B.S. Xu, Characterization Via Image Analysis of Cross-Over Trajectories and Inhomogeneity in Twin Wire Arc Spraying, *Surf. Coat. Technol.*, 2003, **162**, p 301-108
6. A. Pourmousa, J. Mostaghimi, A. Abedini, and S. Chandra, Particle Size Distribution in a Wire-Arc Spraying System, *J. Thermal Spray Technol.*, 2005, **14**(4), p 502-510
7. D.L. Hale, W.D. Swank, and D.C. Haggard, In-Flight Particle Measurements of Twin Wire Electric Arc Sprayed Aluminium, *J. Thermal Spray Technol.*, 1998, **7**(1), p 58-63
8. A.P. Newbery, P.S. Grant, and R.A. Neiser, The Velocity and Temperature of Steel Droplets During Electric Arc Spraying, *Surf. Coat. Technol.*, 2005, **195**, p 91-101

9. A.P. Newbery, T. Rayment, and P.S. Grant, A particle Image Velocimetry Investigation of In-Flight and Deposition Behaviour of Steel Droplets During Electric Arc Sprayforming, *Mater. Sci. Eng.*, 2004, **A383**, p 137-145
10. I. Gedzevicius and A.V. Valiulis, Influence of the Particles Velocity on the Arc Spraying Coating Adhesion, *Mater. Sci.*, 2003, **9**(4), p 334-337
11. J.J. Fang, Z.X. Li, M. Qian, C.L. Ren, and Y.W. Shi, Effects of Powder Size in Cored Wire on Arc-Sprayed Metalceramic Coatings, ITSC, Beijing, May 14-16, 2007, p. 365-370
12. S. Sampath, X. Jiang, A. Kulkarni, J. Matejicek, D.L. Gilmore, and R.A. Neiser, Development of Process Maps for Plasma Spray: Case Study for Molybdenum, *Mater. Sci. Eng.*, 2003, **A348**, p 54-66
13. I.K. Hui, M. Hua, and H.C.W. Lau, A Parametric Investigation of Arc Spraying Process for rapid mould making, *Int. J. Adv. Manuf. Technol.*, 2003, **22**, p 786-795
14. J.P. Fang, Z.X. Li, J.M. Jiang, and Y.W. Shi, Difference in Particle Characteristics and Coating Properties Between Spraying Metallic and Ceramic Powder Cored Wires, *Trans. Nonferrous Metals Soc. China*, 2007, **17**, p 537-642
15. G. Mauer, R. Vaßen, and D. Stöver, Comparison and Applications of DPV-2000 and Accuraspray-g3 Diagnostic Systems, *J. Thermal Spray Technol.*, 2007, **16**(3), p 414-424